PFC/JA-90-41

CIT Elongation Tradeoffs Studies*

L. Bromberg
J. Wei

October 1990

Plasma Fusion Center
Massachusetts Institute of Technology
Cambridge, Massachusetts 02139

Ninth Topical Meeting on the Technology of Fusion Energy, Sponsored by The American Nuclear Society and the U. S. Department of Energy, Hyatt Regency Oak Brook, Oak Brook, Illinois, October 7-11, 1990.

*This work was supported by the Princeton Plasma Physics Laboratory Subcontract S-02969-A.

CIT ELONGATION TRADEOFFS STUDIES†

L. Bromberg and J. Wei
MIT Plasma Fusion Center, Cambridge, MA 02139

Abstract

Results from a study on the effects of increasing the vertical height of the vacuum chamber of CIT are presented in this paper. The increased vertical height would allow for either larger plasma elongation or increased distance between the x-point and the vacuum vessel.

I. Introduction

The implications on the toroidal and poloidal field systems of increasing the vertical height of the vacuum chamber of CIT is studied. An increased vertical height of the vacuum vessel would allow for either larger plasma elongation or increased distance between the x-point and the vacuum vessel. Increased elongation would increase q at constant plasma current, while increasing the distance between the plasma and the target may facilitate placing a closed divertor.

Few changes were incorporated on the baseline PF system. The height of the poloidal field coils on top of the machine has been increased in order to accomodate the increased vertical height of the toroidal field coils and vacuum vessel, but have not altered the other coils. A goal is to determine whether a set of coils optimized for one set of parameters (elongation) could be used for different plasma elongations and/or vacuum vessel height.

Static equilibria for start-up, beginning of flat top (BOFT) and end of flat top (EOFT) have been calculated for several cases, including for the baseline plasma (elongation = 2 at the 95% surface) but with designs with half-height increments of 0.2 m, 0.4 m and 0.6 m. Results of increased plasma elongation, up to 2.4 are also presented.

The organization of this paper is as follows: in section II the plasma stationary equilibria for start-up, beginning of flat top (BOFT) and end of flat top (EOF) are described. This has been done for the baseline plasma (elongation = 2 at the 95% surface) but with designs with half-height increments Δ_h of 0.2 m, 0.4 m and 0.6 m.

† Supported by Princeton Plasma Physics Lab. Subcontract S-02969-A.

In section III, results are presented for a case in which the vacuum vessel half-height has been increased by $\Delta_h = 0.2$ m, and with an x-point 0.05 m from the divertor target (x-point height increased by $\Delta_x = 0.3$ m higher than in the baseline case).

In section IV, the poloidal field system power and energy for the various equilibria are compared. In section V, the out-of-plane loads and the corresponding out-of-plane shears of the toroidal field coil are calculated. In section VI the implications of increased elongation and/or height of the vacuum vessel on the plasma vertical stability is considered. Finally, the conclusions are presented in section VII.

II. Baseline plasma equilibria for increased height of TF coil.

Figure 1 shows the plasma and poloidal field coil location of the baseline configuration (from the CIT System Design Document, SDD)[1]. The details of the poloidal field system have been obtained from a case[2] of the wedged magnet. The major and minor radii are 2.1 and 0.646 m, the toroidal field is 10 T and the plasma current is 11 MA.

In this section the sensitivity of the equilibria configuration to the location of PF4 and PF5 is analyzed (see Figure 1 for the identification of the poloidal field coils). The height of PF4 and PF5 has been increased by 0.2 m, 0.4 m and 0.6 m (corresponding to increments in total machine heights of 0.4, 0.8 and 1.2 m respectively).

The plasma poloidal flux contours for the different cases are superimposed in Figures 2 through 4. The plasma parameters are held constant while the height of PF4 and PF5 is increased. Startups for the four cases (baseline height, 0.2, 0.4 and 0.6 m increased PF coil location) are shown in Figure 2. Figure 3 shows the results for BOFT (beginning of flat top). Figure 4 shows the results for EOFT (end of flat top).

In Figures 2-4, the size of the coils is directly proportional to the amount of current flowing through the coil. They do not correspond to the physical size of the coils. The direction of the current can be determined in Figures 2-4 by the presence or absence of crosses in the coils.

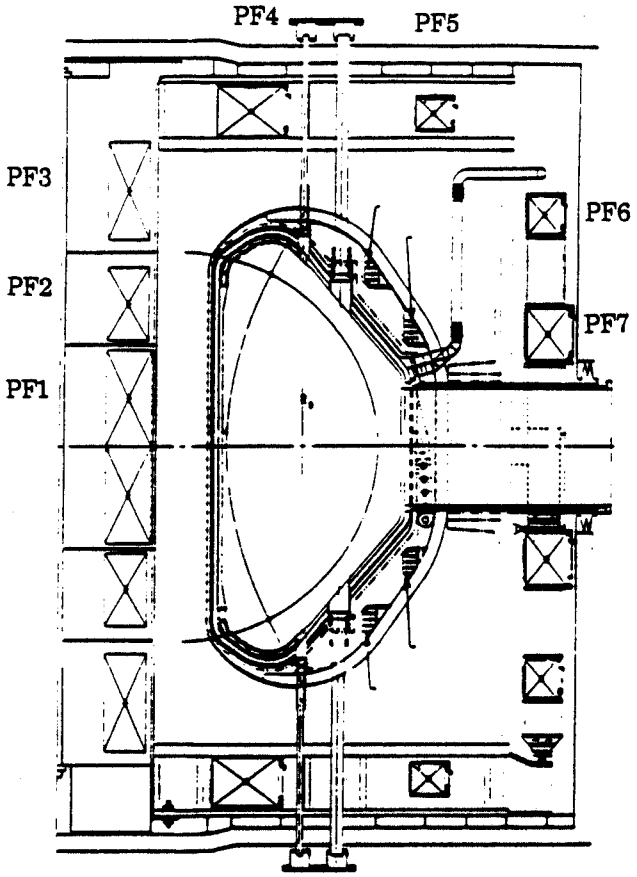

Fig 1. Elevation view of CIT design. System Design Document drawing

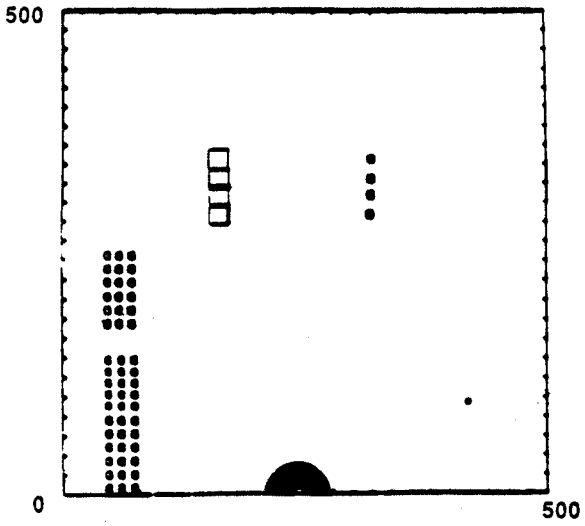

Fig 2. Equilibria for 0408 startup. Δ_h= 0., 0.2 m, 0.4 m and 0.6

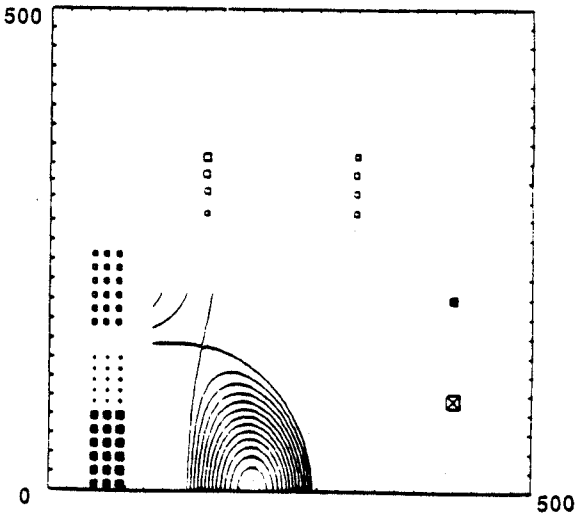

Fig 3. Equilibria for 0408 BOFT. Δ_h= 0., 0.2 m, 0.4 m and 0.6

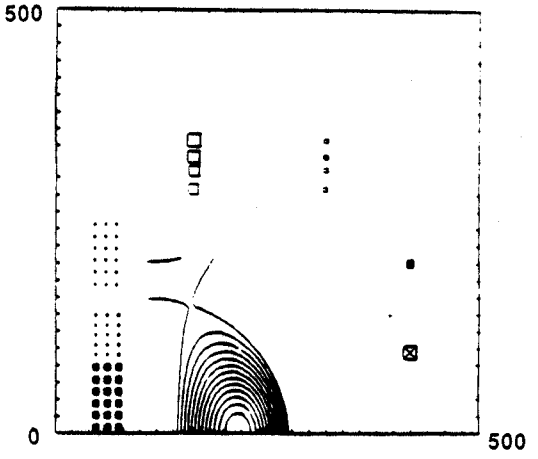

Fig 4. Equilibria for 0408 EOFT. Δ_h= 0., 0.2 m, 0.4 m and 0.6

Increasing the plasma-PF4 coil separation has little effect on the currents in PF4 and PF5. This surprising result indicates that most of the plasma shaping is done by PF1-PF3. The current in PF1 has been kept constant, since PF1 is already at the temperature and heating limits. The only change from increasing the height has been a small reduction of the volt-seconds at startup for Δ_h = 0.2 m, made up by increasing the flux swing between the beginning and end of flat top. For the case of Δ_h = 0.4 m, the PF system actually delivers slightly more inductive flux than the baseline PF.

III. Increased plasma elongation equilibria with increased vacuum vessel height

In this section, results from increasing the plasma elongation while keeping the constant plasma current (i.e., increasing the value of q) are presented. The plasma inductance is lower than in the baseline case due to the increased elongation. Therefore, required flux linkage was decreased by 2 Volt seconds.

Figure 5 shows typical results for the case in which the height of the x-point is increased by $\Delta_z = 0.20$ m. The height location of the poloidal field coils has also been increased by 0.20 m toaccommodate$\Delta_h = 0.2$ m. Therefore, the x-point to divertor target geometry is similar to that of the baseline. To study the effect of sweeping the x-point on the poloidal field system, the plasma triangularity has been varied. The radial locations of the x-point are 1.73 m in Figure 5(a) and 1.90 m in Figure 5(b), corresponding to a radial sweep of the x-point of $\delta r_{sweep} = 0.17$ m. In order to decrease the radial location of the x-point (increase the triangularity) the current in PF4 is increased and the current in PF5 is decreased. Large changes in the location of the x-point are possible with small modifications of the currents in these two coils.

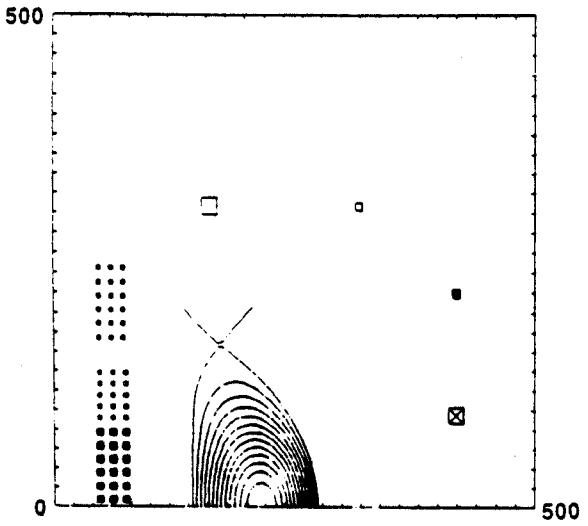

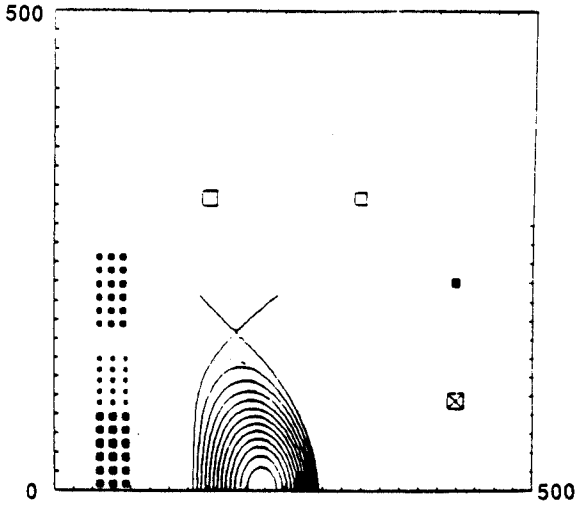

Fig 5. Equilibria for $\Delta_h = 0.2$ m, $\Delta_z = 0.2$ m, for different radial position of the X-point: a) 1.73, b) 1.90 m.

If the plasma elongation is increased to $\Delta_z = 0.3$ m, a suitable divertor with $\Delta_h = 0.2$ m has been difficult to obtain without modifying the poloidal field system. The baseline PF coil system produces plasma equilibria with substantial amount of indentation. With increased elongation, the pulling from PF2 increases and bean shaped plasmas are formed.

To produce a more CIT-like divertor, the PF3 coil was split into two sets of coils. PF3 is the most easily accessible coil of the OH stack. Figure 6 shows the results for the case with split PF3. The radial location of the x-point is 1.85 m for Figure 6(a) and 1.95 m for Figure 6(b), corresponding to $\delta r_{sweep} = 0.10$ m. The x-point in this cases is about 0.05 m from the divertor target.

The current in the upper part of PF3 has increased. Again, to sweep the x-point the current shifts from PF5 to PF6 (the coils are renamed because of the introduction of a new coil).

The location of the PF coils for the baseline have been determined from an optimization for a plasma elongation of 2 at the 95% flux surface. Although appropriate for operation for $\kappa_{95} = 2.2$, it is not appropriate for larger elongations. If larger elongations are desired (x-point very near the baseline divertor target) additional flexibility should be provided for the PF system. The chosen modification (splitting PF3 into two separate coils) may not be the optimal. It has been the intent of this work to show that it can be done with relative ease, without fully optimizing the design.

IV. Calculations of power/energy.

In this section the power and energy of the cases discussed above are presented.

The calculations are referred to the 0408 case[2]. It is assumed that the inconel is at the same temperature as the copper. Table 1 shows the results for the baseline case and the cases with Δ_h = 0.2 and 0.4 m, using the equilibria described in section II. There is very little effect on both the energy and the power of increased vacuum vessel elongation, a consequence of the fact that central stack (PF1, PF2 and PF3) is mainly responsible for the shaping.

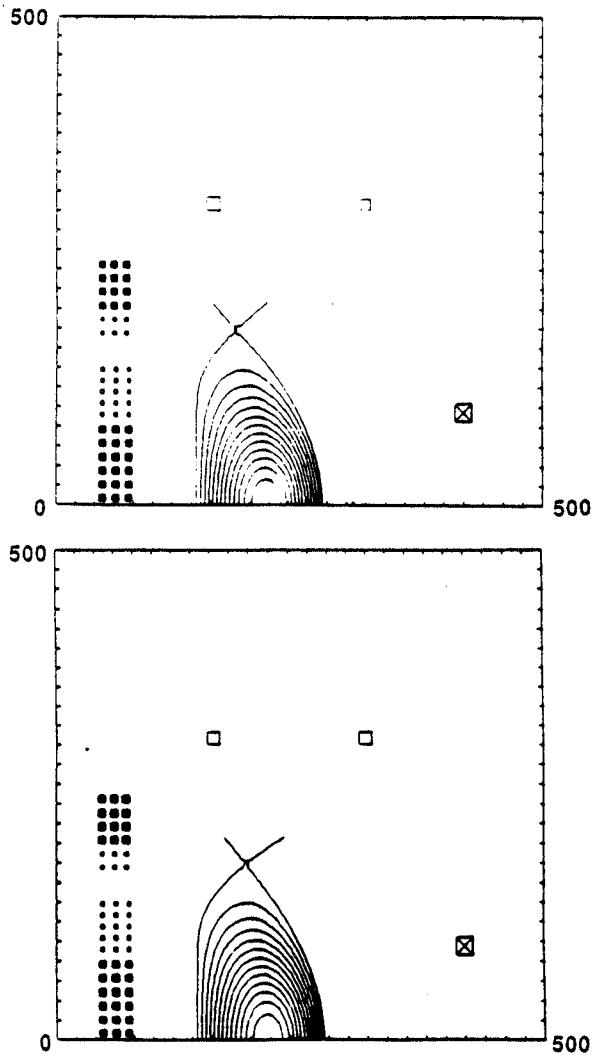

Fig 6. Equilibria for Δ_h = 0.2 m, Δ_z = 0.3 m, for different radial position of the X-point: a) 1.85, b) 1.95 m.

Table 1 also summarizes the results for the cases with Δ_z = 0.2 and 0.3 m. The case with Δ_z = 0.2 m corresponds to the equilibria shown in Figures 5(a) and 5(b) for the flat top (δr_{sweep} = 0.17 m) and the equilibria for Δ_z = 0.3 m (corresponding to a 0.05 m gap between the x-point and the divertor target) are shown in Figures 6(a) and 6(b) (δr_{sweep} = 0.1 m). The power for the Δ_z = 0.2 is about the same as in the case of smaller plasma elongation shown in Table 1, but the energy has increased by a moderate 200-300 MJ.

The reason for the large increase in energy and power between the cases with Δ_z = 0.2 m and Δ_z = 0.3 m is because of the decrease in current in PF6 (Figure 5) as Δ_z is increased. The current in the main equilibrium coil (PF7 in Figure 5) increases. The larger temperature excursion of this coil is reponsible for the substantial increase in power and energy. It should be possible to bring the situation close to that of the smaller elongation by shifting the equilibrium currents between these two coils and reoptimizing the coils.

V. Out-of-plane considerations

In this section, the TF out-of-plane loads for the several cases discussed above are compared.

A simple code has been used to calculate the shear produced in the wedged toroidal field coil by the PF-TF interaction[3]. The model used is based on the orthotropic toroidal thick-shell model, treating the magnet assembly as a thick, continuous orthotropic shell. The thickness of the magnet and the elastic moduli (allowed to be different in two directions) are allowed to vary along the length of the magnet. The treatment is axisymmetric, but by appropriately changing the moduli along the shell it is possible to study the global effects of ports. Stress concentrations would require a full 3-d analysis, beyond the scope of this work.

The results from this code are approximate, and only the global results are presented. In particular, the effects of field variation across the thickness of the magnet are not included. The global behavior and the trends, however, are reasonably well represented with this code.

The shear stresses are calculated for the start-up, BOFT, EOFT and current-conserving disruption (plasma current disappears while the PF coil currents remain constant) at the BOFT. Table 2 summarizes the results. $r_{tapered}$ is the distance along the coil where the coil turns lose contact with the adjacent turns. τ_{max} and τ_{min} are the maximum and the minimum shear stresses, while r_{max} and r_{min} are the locations along the coil where maximum and minimum are located, respectively.

Table 1
PF System Characteristics

	Baseline				
Increased half height Δ_h (m)	0	0.2	0.4	0.2	0.2
Increased x-point height Δ_x (m)	0	0	0	0.2	0.3
Maximum Energy (Stored and Dissipated)					
Time of Max. Energy (s)	26.26	26.26	26.26	26.26	26.26
Stored Energy (MJ)	270	315	387	380	315
Dissipated Energy (MJ)	3150	3275	3340	3450	4800
Total Energy (MJ)	3400	3590	3730	3850	5100
Max. Store Energy(MJ)	930	975	990	1110	1130
Max. Dissipated Energy(MJ)	3210	3370	3440	3550	4890
Peak Power					
Time of Peak Power (s)	13.76	6.0	6.0	13.76	13.76
Magnetic Power (MW)	265	325	330	280	365
Resistive Power (MW)	177	125	125	180	295
Peak Power (MW)	440	450	456	460	660
Flux Swing					
Start-Up Flux (V-s)	23.2	23.0	23.7	23	23
EOFT Flux (V-s)	-30.3	-30.6	-30.4	-28.6	-28.3

Table 2
Toroidal Field Coil Shear Stresses

	$r_{tapered}$ (m)	τ_{max} (MPa)	r_{max} (m)	τ_{min} (MPa)	r_{min} (m)
$\Delta_x = 0$, $\Delta_h = 0$					
start-up	2.1	12	1.4	-18	2.5
BOFT	2.1	30	0.4	-45	2.0
EOFT	2.1	38	0.3	-35	1.9
BOFT-disruption	2.1	48	0	-65	2.0
$\Delta_x = 0$, $\Delta_h = 0.2$					
start-up	2.3	15	1.4	-34	2.6
BOFT	2.3	42	0.4	-40	2.0
EOFT	2.3	42	0.3	-35	2.1
BOFT-disruption	2.3	65	0	-57	2.1
$\Delta_x = 0.2$, $\Delta_h = 0.2$					
start-up	2.3	13	1.5	-18	2.7
BOFT	2.3	35	0.4	-30	2.6
EOFT	2.3	30	0.4	-30	2.6
BOFT-disruption	2.3	53	0	-40	2.5
$\Delta_x = 0.3$, $\Delta_h = 0.2$					
start-up	2.3	15	1.5	-18	2.7
BOFT	2.3	30	0.4	-20	2.7
EOFT	2.3	32	0.3	-23	2.7
BOFT-disruption	2.3	53	0	-38	2.4

Figure 7 shows, for the inner and outer chords of the magnet, the shear stresses as a function of the distance along the magnet starting at the inboard midplane, calculated at BOFT current conserving disruptions. The baseline case (Fig. 7(a)), and the cases with $\Delta_h = 0.2$ m with $\Delta_x = 0$ (Fig. 7(b)) and $\Delta_x = 0.2$ m (Fig. 7(c)) are shown.

The shear stresses in the upper inner leg are slightly larger in the case of elongated vacuum vessel with a baseline plasma. However, the shears are reduced to comparable levels in the case of $\Delta_h = \Delta_x = 0.2$ m. There are substantial stresses in regions where there is little support by wedging. Therefore the ability of carrying out-of-plane loads by wedging in that area is still a reason for concern, and does not change appreciably as the vacuum vessel height is increased.

VI. Vertical stability considerations

Highly elongated plasmas are susceptible to a vertical instability. Passive conductors and the vacuum vessel slow down the growth of the mode. Passive stabilizers do not completely stabilize these modes since the stabilizing currents decay. The resistive diffusion time is $\tau_D = \frac{\mu_0 b d}{\eta}$, where b is a measure of the minor radius of the vacuum chamber and d is the thickness. For CIT, $b \sim 0.66$ m, $d \sim 0.067$ m, and $\eta \sim 1.3 \times 10^{-6}$ Ω m, $\tau_D \sim 4.3 \times 10^{-2}$ sec. This value is in approximate agreement with more detailed calculations, with $\tau_D \sim 5.6 \times 10^{-2}$ s, performed by Kessel and Jardin[4].

The vertical stability of the plasma has been analyzed using a simplified model[5]. The plasma boundary is chosen at the 95% flux surface and the plasma equilibrium is determined by the variational method. Figure 8 shows the plasma surface and the filamentary model of the vacuum vessel. Since the most unstable modes tend to be mainly vertical and incompressible, the plasma displacement is written in the form,

$$\xi(\mathbf{r},t) = \xi_z(R)e^{\gamma t}\mathbf{e_Z},$$

with

$$\nabla \cdot \xi = 0$$

where ξ is the displacement (assumed to be in the vertical direction), γ is the growth rate, R is the distance from the major axis and $\mathbf{e_Z}$ is in the vertical direction. This assumption, which considerably simplifies the analysis, allows for an R dependence of the vertical displacement eigenmodes $\xi_z(R)$. This model is an improvement with respect to the rigid displacement model. The model uses the extended energy principle to estimate the resulting growth rate for a system without a perfectly conducting wall.

Four cases have been studied. The results are shown in Table 3. The growth rate for the case of both elongated plasma and increased vacuum vessel height is almost three times larger than that of the baseline design, making the vertical plasma control more demanding.

Section VII. Conclusion

It has been shown that increasing the height of the vacuum vessel has little effect on the characteristics of the poloidal field system for the baseline plasma. The implication is that the coils in the throat of the magnet are mainly responsible for the shaping. If elongation greater than $\kappa_{95} = 2.2$ are desired, the poloidal field system should be reoptimized. The out-of-plane behaviour of the toroidal field coil has been found not to be sensitive to increased elongation of the vacuum chamber. The vertical stability of the plasma has been analyzed, and not surprisingly, it has been determined that the growth rate of the vertical stability increases by about a factor of three if the elongation and the vacuum vessel height are increased.

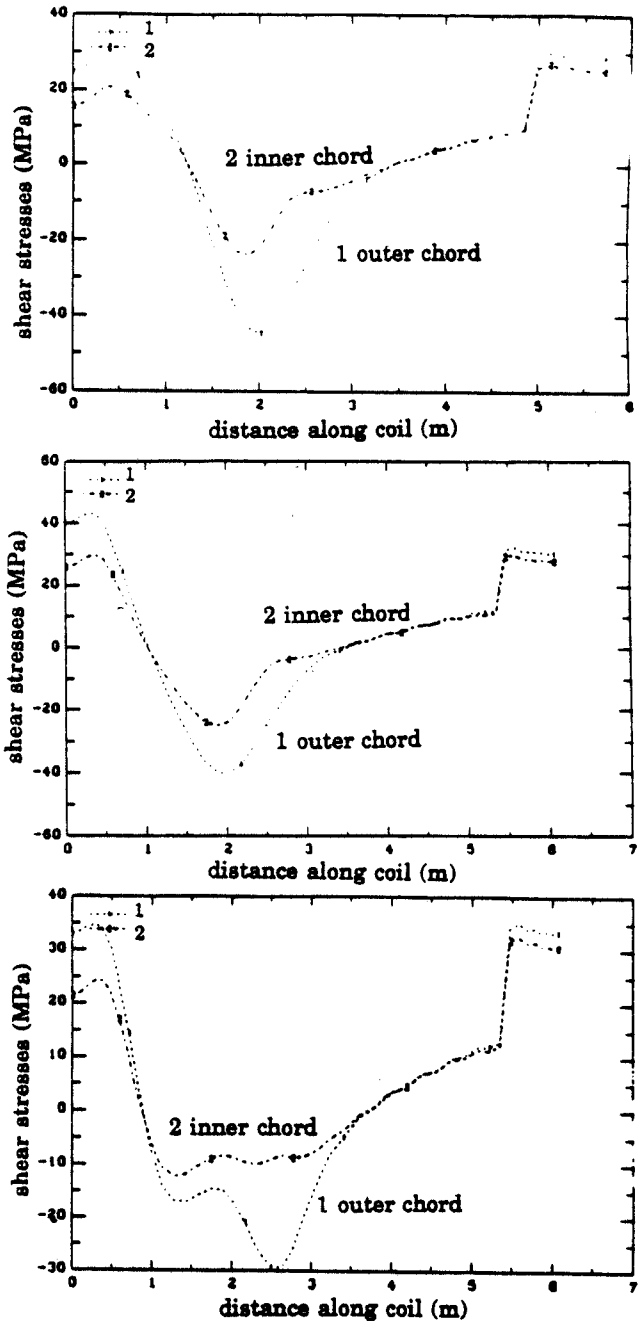

Fig 7. Shear stresses in the inner and outer fibers for a current conserving disruption during BOFT: a) baseline; b) $\Delta_h = 0.2$ m, $\Delta_s = 0$; c) $\Delta_h = 0.2$ m, $\Delta_s = 0.2$

References

[1] CIT Design Team, "System Design Document, Compact Ignition Tokamak", Report W-881201-PPL-05, December 1 (1988)

[2] R.D. Pillsbury, Jr, "PF System for the CIT 2.1 m Machine", Memorandum MIT-PF040888, April 8 (1988)

[3] E.S. Bobrov, "Structural Response of Tokamak TF Magnet Systems to In-Plane and Out-of-Plane Electromechanical Loads", *Nucl. Engineering and Design/Fusion*, Vol 1, p 39-50 (1984)

[4] C. Kessel and S. Jardin, CIT Report AE890609-PPL-01 (1989)

[5] Haney, S.W., and Freidberg, J.P., "Variational Methods for Studying Tokamak Stability in the Presence of a Resistive Wall, Phys. Fluids, Vol. 1, 1637 (1989)

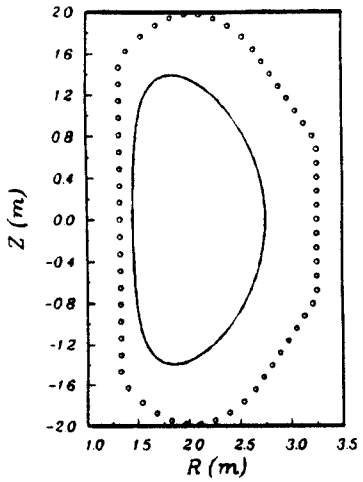

Fig 8. Plasma and vacuum vessel model for the calculations of the vertical instability

Table 3
Growth Rate of the Vertical Stability

Δ_h (m)	Δ_z (m)	γ (Hz)
0	0	99
0.2	0	140
0	0.2	160
0.2	0.2	270